Naval Structural Antenna Systems for Broadband HF Communications—Part II: Design Methodology for Real Naval Platforms

Gaetano Marrocco, *Member, IEEE*, Lorenzo Mattioni, and Valerio Martorelli

***Abstract*—Recently, it was shown how to make a multipurpose broadband HF antenna system out of existing naval superstructures such as the funnel or a big mast. The idea was discussed by means of canonical structures, e.g., a cylindrical body of circular or square cross-section, placed onto an infinite ground plane. This paper investigates the critical aspects concerning the extension of naval structural antenna concept to real ship platforms with the aim to define a general design methodology for impedance matching and radiation pattern control. The method is described with reference to a realistic frigate model, whose big mast is transformed into a broadband HF antenna system able to perform communications by both sea-wave and sky-wave links. It is demonstrated that, even in a real environment, the multiport strategy permits to increase the system efficiency and to moderately shape the radiation pattern in order to overcome the shadowing effect due to other large objects.**

***Index Terms*—Broadband antennas, HF antennas, loaded antennas, naval communications, software defined radio, structural antennas.**

I. Introduction

THE advances in software defined radio technology [1]–[3], demand broadband radiating systems in the 2 MHz–2 GHz frequency range. Since most of the new applications will be embedded into avionic, naval and also auto-vehicular platforms, new antenna problems need to be addressed in order to obtain highly-performance equipments within a limited space. One of the most challenging designs concerns the HF domain where the antenna resonant length could be of similar size as the whole platform [4]–[6]. Therefore a strong pattern distortion [7] and source mismatch may occur due to the field interaction with the environment, demanding multiple antennas and encouraging *ad-hoc* solutions [8].

Recently, the authors have introduced the concept of naval structural antenna (NSA) [9], [10] which consists in transforming a portion of the naval platform such as a funnel or a big mast into a part of a true integrated broadband multiport radiating system. The interactions of the HF source with a part of the ship, which in general produces undesired effects, are instead steered to give unconventional performances and to reduce the number of antennas onboard. This idea was investigated with reference to canonical geometries over a perfect ground plane (Fig. 1), but some important topics were however left open, such as the real feasibility of the NSA concept in a real crowded naval platform, and the recovering of possible port mismatch, at some frequencies, caused by the high inter-port coupling.

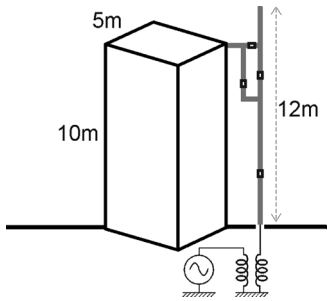

Fig. 1. Example of a structural antenna system with a square cross-section central body, resembling a funnel or a big mast, fed by loaded wires.

In this paper, the critical aspects concerning the extension of the NSA concept to a realistic ship environment will be investigated with the purpose to define a general ship-suited design strategy. The discussions and the methodologies will be referred to a realistic ship model resembling a frigate where the challenge is to transform the big central mast into a broadband multiport HF antenna system with a really limited use of the available space. The considered scenario is rather common and therefore the design methodology which will be developed, although experimented with a benchmark ship, is of general interest and can be extended to several installation typologies.

The paper opens (Section II) with the definition of reference performance indicators for on-board HF naval antennas and introduces the optimization problem for loaded broadband antennas including the ship superstructures. Section III gives details about the design of a single-port structural antenna (NSA_1) *on the mast* by a modification of the wire radiators in [9], for what concerns the position and values of the loading impedances. Then, the 4-port (NSA_4) extension is considered in Section IV with attention to the embedded patterns features and to the resulting system efficiency. Finally, a pattern synthesis optimization problem is formulated in Section V, with the additional constraint of the impedance matching at the antenna ports. By a proper control of port amplitudes and/or phases, it is hence demonstrated how to improve the pattern uniformity at the horizon, caused by the distorting effect of

Manuscript received May 22, 2006; revised June 22, 2006. This work has been funded by SELEX Communications, a Finmeccanica Company.

F. Marrocco and L. Mattioni are with the Dipartimento di Informatica, Sistemi e Produzione, University of Roma "Tor Vergata," Roma 00133, Italy (e-mail: marrocco@disp.uniroma2.it).

V. Martorelli was with the University of Roma "Tor Vergata," Roma 00133, Italy. He is now with the Istituto Nazionale di Astrofisica di Bologna, 40127 Bologna, Italy.

Digital Object Identifier 10.1109/TAP.2006.884306

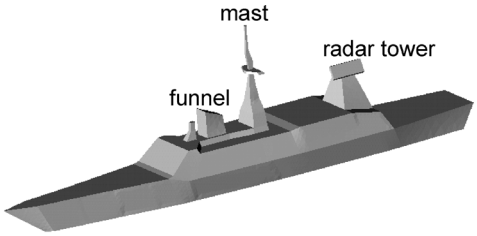

Fig. 2. Simplified model of a frigate where the NSA concept will be experimented. The ship is 120 m long and 15 m wide.

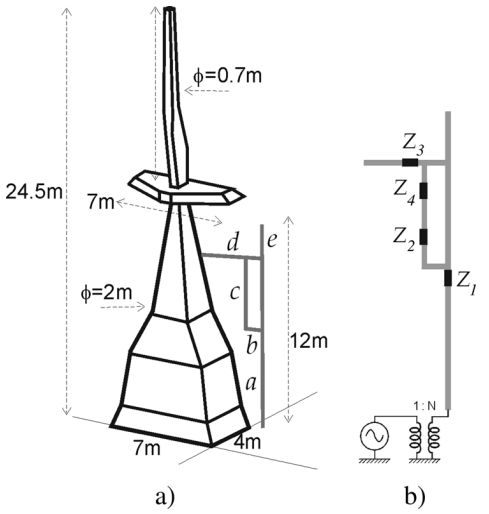

Fig. 3. (a) Transforming the mast into an NSA_1 by loaded-wires feeding. Size are: $a = 6$ m, $b = 1$ m, $c = 4$ m, $d = 3.5$ m, $e = 2$ m. (b) Loading impedances optimized by GA for the case of the mast over a perfect ground: Z_1 is the series connection of $L_1 = 0.23\ \mu$H and $C_1 = 506$ pF; Z_2 is the series connection of $L_2 = 0.77\ \mu$H and $C_2 = 561$ pF; Z_3 and Z_4 are resistors of value 54 Ω and 9 Ω. The impedance transformer ratio is $N = 4$.

the surrounding deck objects, and how to enhance the system radiation toward a given angular sector having all the ports matched with $\mathrm{VSWR} < 3$.

II. Statement of the Problem

The reference naval platform, considered to illustrate the design methodology, is a typical frigate-like geometry (Fig. 2) containing a big mast, a funnel and a radar tower. The mast to be turned into an antenna is enlarged in Fig. 3(a). The nonuniform cross-section, tapered from the ground to the top, ranges from 7 m $\times$ 4 m at the base, to 0.7 m $\times$ 0.7 m at the top, and the overall height is more than twice the size of the canonical cylinders (height 10 m) previously considered by the authors [9]. In analogy with Fig. 1, the mast becomes one of the vertical conductors of a folded-monopole like geometry, and the wires are loaded by lumped electric circuits [9]. Based on the previous experience, the same wire geometry as in the cylindrical NSA structure of Fig. 1 is connected to an edge of the mast while the loading circuits have to be re-optimized for what concerns topology, position and electrical values, by a genetic algorithm optimization as in [9], [11] and [12].

The performances to be met are partly borrowed from [8] and [13], e.g.:

- $\mathrm{VSWR} < 3$ (line impedance 50 Ω);
- Averaged gain at the horizon ($\theta = 90°$) more than -10 dB for $2\ \mathrm{MHz} \le f \le 5\ \mathrm{MHz}$ and higher than 2 dB above 5 MHz;
- Averaged gain at high elevation angles ($\theta = 10°$) more than -20 dB to achieve Near Vertical Incidence Skywave (NVIS) communications;
- Gain variation on the horizontal plane with respect to the peak value, less than 10 dB in the 80% of the whole azimuthal angle. The functions $U(f)$ and $\bar{U}$, referred to as *pattern uniformity* [see Appendix, (7)] and *global pattern uniformity*, respectively, indicate the percentage of the whole azimuthal angle at the frequency f, and the percentage of the whole band ($\bar{U}$), where the gain requirement is met.

In the given examples, all the objects are considered made of aluminium and the wires are 10 cm-cross-section pipes. The electromagnetic models of the mast equipped with wires and of the surrounding environment required for the GA optimization are achieved by method of moments (MoM) [14]. More in detail, the mast and the ship are modelled by surface current basis functions, while the wires by one-dimensional basis functions. In the second half of the band (20–40 MHz), the huge size of the unknowns requires a combined MoM and multilevel-fast-multiple-multipole approach [15]. The sea is modelled as a perfect ground plane.

III. Design of NSA On-the-Mast

The considered problem is a rather hard challenge since additional difficulties are now present in comparison with the simplified structures in [9] due to the high extension of the mast, to the absence of azimuthal periodicity as in a cylinder, and to the interactions with large objects on the ship, such as the funnel and the radar tower placed at a close proximity to the mast. To isolate the features of the *mast-as-antenna* from the interactions with the ship environments, a preliminary optimization assumes the mast to be placed over a perfect ground plane. Since the overall height of the wire radiator is 12 m, it is expected that the current over a consistent portion of the mast, from the horizontal platform up to the tip, will be out of any control. By previous experiences, having fixed to four the maximum number of loading impedances, the optimizer selected two series LCs and two resistors placed as in Fig. 3(b) and a nearly omnidirectional pattern is obtained with variations smaller than 10 dB in the most part of the band (global uniformity $\bar{U} = 87\%$). The other results are shown in Fig. 4. Besides a good matching in the whole HF band, it can be observed that the ϕ-averaged gain at the horizon reduces around 8 MHz. At this frequency, the mast electrical height, including the overlength due to the horizontal platform, is roughly λ, and the current exhibits two oscillations. The upper part of the mast radiates with a 180° phase difference with respect to the current on the wires and on the lower part of the mast, and therefore the gain at the horizon is lowered. To overcome this problem, some choke mechanisms could be introduced in the upper part of the mast with the purpose to suppress, or at least to reduce, the induced currents as in [16]. In the following part of the paper an unchoked mast is nevertheless considered since, as shown later on, the multiresonance

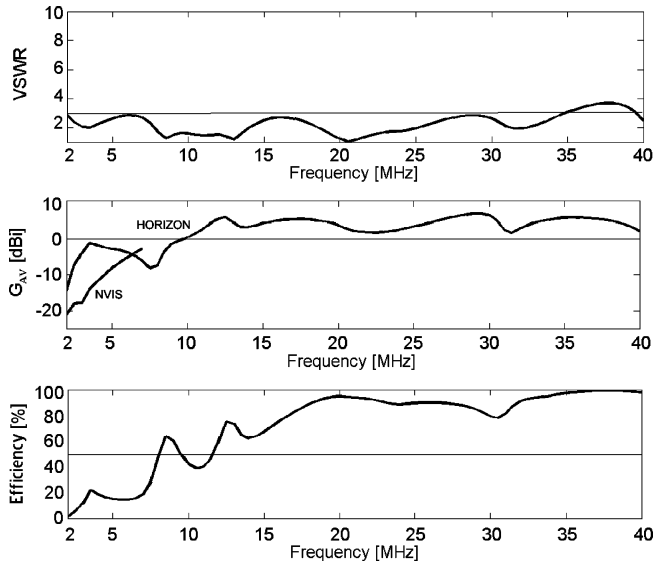

Fig. 4. NSA_1 over a perfect ground plane. VSWR, ϕ-averaged gain at the horizon and at NVIS ($\theta = 10^\circ$), and efficiency.

behavior of the mast is less effective when the NSA is installed on the ship due to the interactions with the naval structure.

When the NSA_1 without chokes, and provided with the loads optimized in the perfect ground configuration, is placed in the real position over the ship, some changes in the antenna features occur due to the electromagnetic coupling with the surrounding environment. The VSWR (Fig. 5, dashed line) reveals a slight mismatch at low frequencies ($\mathrm{VSWR} < 4$), while the ϕ-averaged gain does not any longer exhibit the reduction around 8 MHz, as in the perfect ground case. After a new optimization of a same number of loads, involving the full electromagnetic model of the antenna together with the naval platform, the NSA_1 becomes well matched in the whole HF band (Fig. 5, solid line). Nevertheless, because of the ship-to-sea discontinuity and the presence of other deck objects, such as the funnel and the radar tower (Fig. 2), the global pattern uniformity gets worse ($\bar{U} = 70\%$) with respect to the perfect ground case (it was $\bar{U} = 87\%$). The most penalized frequencies, in the HF band, are close to 8 and 28 MHz.

IV. Design of Multiport Configurations

The multiport configurations (NSA_N) require that multiple wires and feed points are connected to the central thick superstructure (the mast in the reference geometry). The resulting arrangement should minimize the coupling of the wire conductors with the surrounding deck objects. Fig. 6 shows an example of NSA_4 on the frigate, where the wires share the same loading set (topology, values and positions) of the NSA_1 on the ship. Additional degrees of freedom could be included if the loading impedances of each wire were independently chosen at the cost of a not negligible increase in the optimization times.

This system can be used in *incoherent* (multichannel) mode, where each port is instantaneously allocated to a single channel, or in *coherent* (mono-channel) mode where all the ports are instantaneously allocated to a single channel.

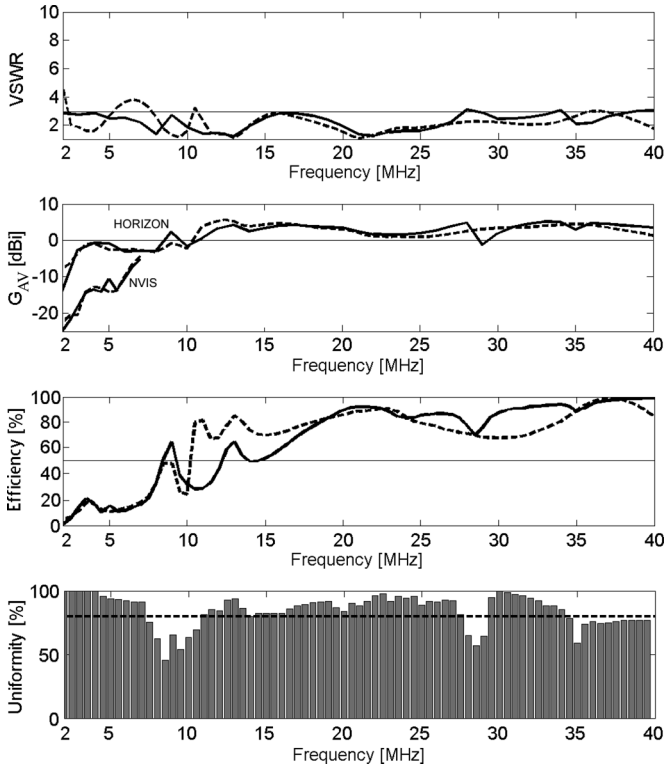

Fig. 5. NSA_1 on the ship. VSWR, ϕ-averaged gain at the horizon and at the NVIS ($\theta = 10^\circ$), and efficiency. Dashed lines tag the performances with loading impedances borrowed from the mast-plus-perfect ground model, while continuous lines refer to the case where the loading impedances are those re-optimized for the must-plus-ship model. The histogram describes the pattern uniformity $U(f)$ referred to 10 dB gain difference from the peak value.

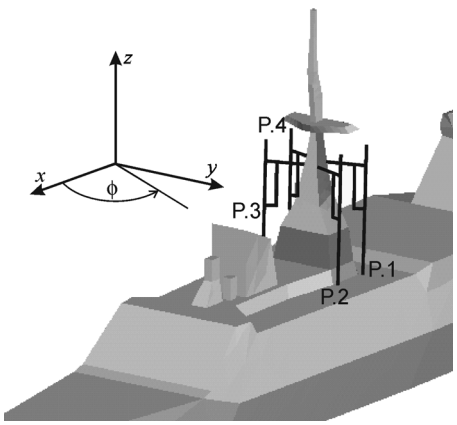

Fig. 6. NSA_4 on the ship. The four wire radiators are connected to the mast edges.

The incoherent management of the NSA_N for a realistic installation is here discussed, while the coherent case is addressed in the next section.

The independent excitation of the antenna ports to host multiple channels at a same time without the use of signal combiners is feasible if i, the radiation patterns of the system, when a single port is fed (*embedded*[1] radiation pattern), retain reasonable omnidirectional features and ii) the excited port is still

[1]The embedded radiation pattern is calculated as the gain radiated by the whole NSA_4 when only a port is sourced while the others are connected to the line load (200 Ω). The embedded VSWR and efficiency are obtained in the same conditions.

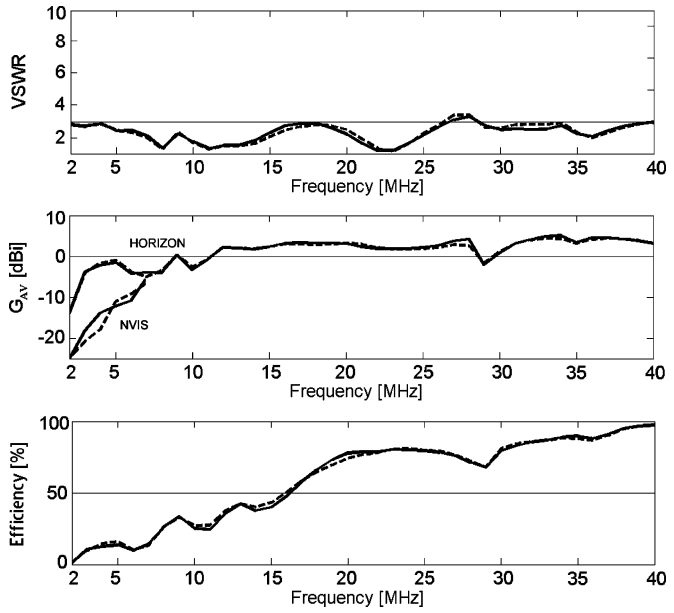

Fig. 7. NSA_4 on the ship. Embedded VSWR, ϕ-averaged gain and efficiency. Due to the nearly simmetry with respect to the xz-plane of the geometry and the scenario (Fig. 6), curves related to port $P.1$ (continuous lines) and port $P.2$ (dashed lines) are completely superimposed to those of port $P.4$ and port $P.3$, respectively.

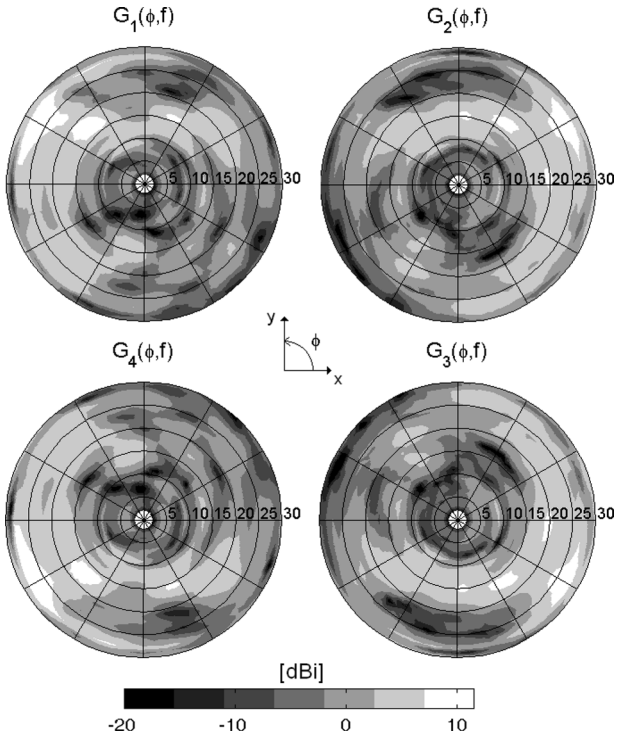

Fig. 8. NSA_4 on the ship. Embedded gain patterns at the horizon related to each port. Labels on the horizontal axis tag the frequency. Since the ship is almost symmetrical with respect to $\phi = 0^\circ$ (corresponding to the ship bow), G_3 and G_4 are the mirror image of G_2 and G_1, respectively.

matched. It has been verified that also for the NSA_4 on the ship the embedded VSWR at the system ports remain well matched in the whole HF band (Fig. 7). When compared with diagrams of Fig. 5, referring to the NSA_1 performances, the NSA_4 embedded average gain and efficiency show similar values in the most part of the HF band. This means that an improvement in the system efficiency of about four times [9] can be theoretically achieved when four channels are simultaneously allocated to the NSA_4, one for each port, instead of using the NSA_1 equipped with a 4:1 signal combiner.

The embedded radiation patterns, nevertheless, deserve some discussions. By the geometrically symmetry with respect to the xz-plane, the embedded element factors associated with port $P.1$ and port $P.2$ are mirror images of ports $P.4$ and $P.3$, respectively (Fig. 6). However, due to the strong interactions among wires, the overall pattern uniformity of each port is worse than the NSA_1 arrangement ($\bar{U} = 40\%$ instead of 70%) and some blind directions appear at different angles and frequencies depending on the excited port (Fig. 8). The versatility of a NSA_N on a real ship, as multichannel system, is hence reduced in comparison with the ideal case of the perfect ground plane since the channels need to be properly distributed over the antenna ports taking into account the angular sector relevant to the communication. For instance, if it is required to activate the NSA_4 on the frigate for a communication at 10 MHz along $\phi = 90^\circ$, the port $P.1$ or $P.2$ have to be used since the others have low values of gain, while for communications at 15 MHz along $\phi = -60^\circ$ both $P.3$ and $P.4$ ports can be chosen.

V. Radiation Pattern Shaping

The use of the multiport NSA as an array (coherent mode) promises a moderate degree of pattern shaping with the purpose to improve the gain uniformity or concentrate the radiation toward a given angular sector. Although the NSA_N system can not be considered as a true array [17], since the radiating elements are tightly connected, it is nevertheless expected that different current patterns may be excited depending on the amplitudes and phases at the input ports. The overall radiated field can be expressed in terms of the embedded antenna fields, $\boldsymbol{E}_n(r,\theta,\phi,f)$, as

$$\boldsymbol{E}(r,\theta,\phi,f) = \sum_{n=1}^{N} A_n(f)\boldsymbol{E}_n(r,\theta,\phi,f) \tag{1}$$

where $A_n(f) = C_n(f)e^{j\alpha_n(f)}$, $\{C_n,\alpha_n\} \in \mathbb{R}$, is the excitation of the nth port. Due to the high inter-port coupling, the impedance matching needs to be controlled together with the pattern shaping.

It is here formulated a general multiobjective constrained optimization problem for the solution of the $\{A_n\}$ excitation coefficients in order to achieve different kinds of performances, such as *i*) the excitation of uniform patterns on the horizontal plane, *ii*) the radiation enhancement within a particular azimuthal angular sector and *iii*) the improvement of NVIS radiation. Since it is not possible to extract a true array factor from the total radiated field expression, the optimization is again performed by a GA approach controlling not only the pattern shaping and the number of the excited ports, but also the port matching.

Coupling-constrained array pattern synthesis have received considerable interest starting from the late 1960 [18]. Different techniques [19], [20], have been used to shape the pattern and, at

the same time, to design matching networks able to mitigate the relevant impedance change of the radiating elements in steerable-beam arrays. In the Software Defined Radio context, signal waveforms to be transmitted can be easily managed by the processing unit with the possibility to digitally set their amplitude and phases [21]. The impedance-matching and radiation-pattern constraints optimization can be therefore more easily formulated straight in terms of amplitudes and phases. Additionally, to have the transmitters working with the maximum power, only a phase synthesis will be considered. It is assumed that $C_n = \{0, 1\}$ and, in the general case of N excited ports, e.g., $A_n = e^{j\alpha_n(f)}$, $N-1$ degrees of freedom are available. The multiobjective optimization requires the minimization, at each frequency, of the following penalty function:

$$F = w_S F_S + w_U F_U + w_A F_A + w_V F_V + w_N F_N \quad (2)$$

where, depending on the particular requirements to meet, only some of the weight coefficients $\{w_x\}$ are different than zero. F_S, F_U, F_A, F_V and F_N are the normalized functions $(0 < F_x < 1)$ described in detail in the Appendix, respectively controlling the port matching (F_S), the uniformity of the azimuthal pattern at horizon (F_U), the horizontal gain in a defined azimuthal sector (F_A), the NVIS gain (F_V), and the number of excited ports (F_N). In particular, the F_U function controls the effective average gain, $G_{EFF} = G_{AV}U$, which is a measure of the pattern uniformity weighed by the average gain G_{AV}, that correctly penalizes those patterns which, although uniform in azimuth, exhibit a low average gain.

This multiobjective optimization strategy for the pattern shaping is expected to be more robust than that described in [9] which only compensated the phase differences among the embedded radiation patterns along a given direction and did not account for the port matching.

A. Excitation of Uniform Patterns

A proper choice of the NSA_N phases can mitigate the pattern distortion of the NSA_1 radiator caused by the ship interactions, with the purpose to achieve a pattern uniformity $U(f) > 80\%$. Accordingly, the penalty function (2) is customized by setting $w_V = w_A = 0$. The reference configuration for the evaluation of the uniformity enhancement is the NSA_1 on the frigate corresponding to port $P.1$ which, from Fig. 5 suggests some improvements around 8, 10, 14, and 29 MHz. After the phase optimization, the azimuthal patterns of Fig. 9 are obtained for the NSA_4, having all the excited ports well matched with VSWR < 3. In all the cases the effective average gain G_{EFF} has been highly improved as shown in Table I. The uniformity requirement is met at all the frequencies with a reasonable high ϕ-averaged gain at the expenses of the maximum gain which is generally penalized in favour of a raising of the minimum values. It is finally interesting to note that not all the ports are always excited: for instance at 10 and 28.5 MHz only two of them are required to achieve pattern uniformity. In such a case the remaining ports could be allocated to other services, improving the system flexibility, or dedicated to the same channel with higher performances (for instance, the effective gain at 10 MHz can be improved from $G_{EFF} = -1.8$ dB to $G_{EFF} = 1.2$ dB).

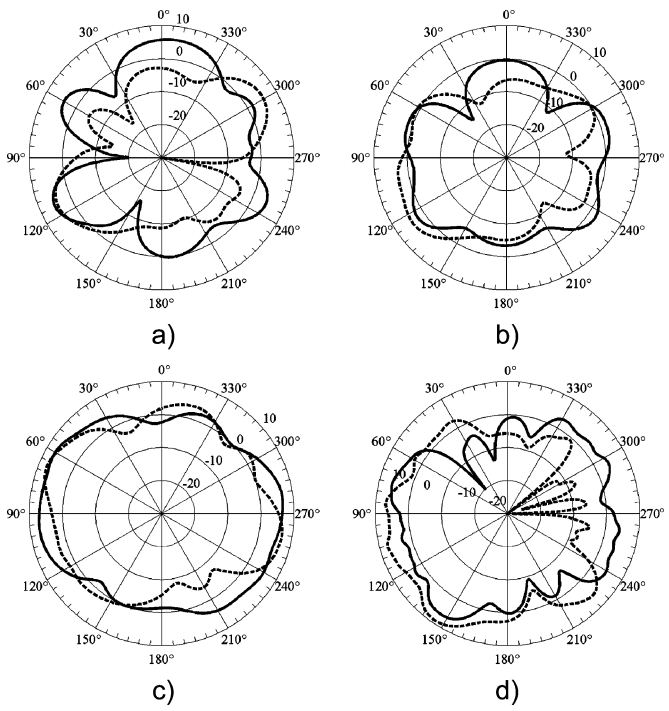

Fig. 9. Phased NSA_4 (continuous lines) for uniform pattern synthesis at the horizon ($\theta_0 = 90°$) compared with the azimuthal gain pattern of NSA_1 corresponding to port $P.1$ (dashed line). (a) $f = 8.5$ MHz, four ports used, $\alpha_1 = 0°$, $\alpha_2 = 24°$, $\alpha_3 = 325°$, $\alpha_4 = 315°$, $1.7 < VSWR < 2.2$. (b) $f = 10$ MHz, two ports used, $\alpha_2 = 0°$, $\alpha_3 = 5°$, $1.5 < VSWR < 1.7$. (c) $f = 14$ MHz, four ports used, $\alpha_1 = 0°$, $\alpha_2 = 296°$, $\alpha_3 = 164°$, $\alpha_4 = 121°$, $1.7 < VSWR < 2.5$. (d) $f = 28.5$ MHz, two ports used, $\alpha_1 = 0°$, $\alpha_3 = 150°$, $3.1 < VSWR < 3.2$. The direction $\phi = 0°$ corresponds to the ship bow. Details about gain improvements in Table I.

TABLE I
GAIN PARAMETERS WHEN THE NSA_4 IS PHASED FOR HORIZONTAL PATTERN UNIFORMITY

		a) 8.5MHz 4 ports	b) 10MHz 2 ports	c) 14MHz 4 ports	d) 28.5MHz 2 ports
G_{MAX} [dB]	NSA_1	5.6	4.5	7.5	9.1
	NSA_4	5.9	2.4	7.2	6.6
G_{AV} [dB]	NSA_1	-4.7	-4.3	1.9	1.5
	NSA_4	0	-1.4	3.8	2
U [%]	NSA_1	45	63	80	57
	NSA_4	85	92	100	80
G_{EFF} [dB]	NSA_1	-8.2	-6.3	0.9	-0.9
	NSA_4	-0.6	-1.8	3.8	1

B. Improving Radiation Within an Angular Sector

To achieve directional properties with the NSA_N *on the mast* at the horizon $\theta_0 = 90°$, within an azimuthal sector centered at ϕ_0 ($|\phi - \phi_0| < \Delta\phi/2$), the penalty function in (2) is customized by setting $w_V = w_U = 0$. This is a hard objective since some blind sub-bands with VSWR > 3 have been experienced in [9]. The effectiveness of the optimization results is quantified by a global indicator $I(\theta_0, \phi_0, \Delta\phi)$ giving the relative increase of the radiated power in that angular sector with respect to the pth

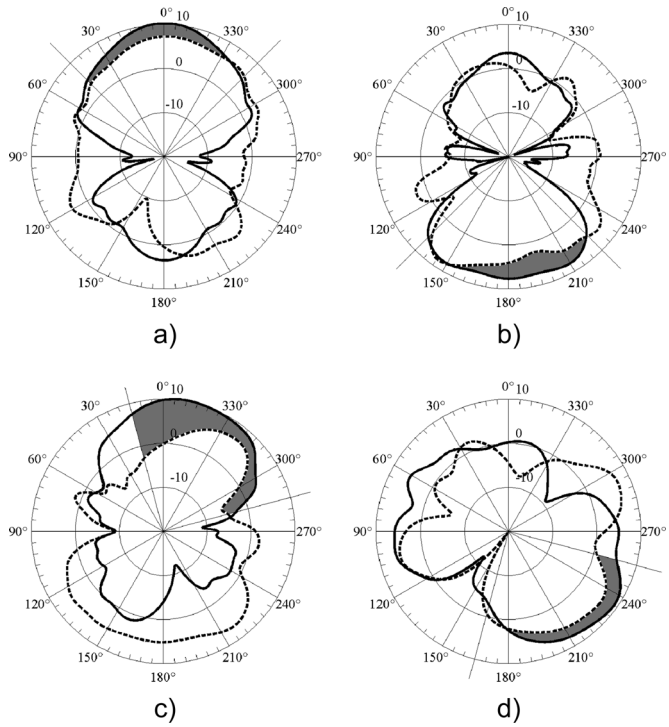

Fig. 10. Phased NSA_4 (continuous lines) for sectorial pattern synthesis at the horizon ($\theta_0 = 90°$) compared with the embedded pattern having the highest gain at ϕ_0 (dashed lines). (a) $\phi_0 = 0°$, $f = 20$ MHz, two ports used, $\alpha_2 = \alpha_3$, $VSWR = 2.6$, $I = 61\%$. (b) $\phi_0 = 180°$, $f = 25$ MHz, two ports used, $\alpha_4 = \alpha_1$, $VSWR = 2.1$, $I = 56\%$. (c) $\phi_0 = 330°$, $f = 20$ MHz, three ports used, $\alpha_4 = 0°$, $\alpha_2 = 297°$, $\alpha_3 = 289°$, $1.6 < VSWR < 3$, $I = 230\%$. (d) $\phi_0 = 210°$, $f = 15$ MHz, three ports used, $\alpha_4 = 0°$, $\alpha_2 = 200°$, $\alpha_3 = 96°$, $2.3 < VSWR < 3$, $I = 66\%$.

embedded pattern having the best gain, G_p, toward the steering direction ϕ_0

$$I(\theta_0,\phi_0,\Delta\phi) = \frac{\int_{\phi_0-\Delta\phi/2}^{\phi_0+\Delta\phi/2} |G_{NSA_4}(\theta_0,\phi) - G_p(\theta_0,\phi)|\, d\phi}{\int_{\phi_0-\Delta\phi/2}^{\phi_0+\Delta\phi/2} G_p(\theta,\phi_0) d\phi}. \tag{3}$$

For the NSA_4 on the frigate, it has been found that the gain improvement is relevant above 15 MHz, where the NSA ports begin to be electrically far enough to produce an array behavior. Additionally, since the embedded gain patterns (Fig. 8) are not azimuthally uniform in the whole HF band, there are some frequencies and angles, for instance $\phi = \pm 90°$, where their radiation is simultaneously low and therefore only negligible gain improvement can be achieved by phasing the NSA_4. Fig. 10 gives some examples of radiation enforcement along the ship bow ($\phi_0 = 0°$) and stern ($\phi_0 = 180°$), and along intermediate directions ($\phi_0 = 330°$ and $\phi_0 = 210°$). The shadowed regions are representative of the radiation power improvement, $I(90°, \phi_0, 90°)$ in $|\phi - \phi_0| < 45°$, ranging from 50% up to more than 200%.

Beyond 30 MHz the mast starts to act as reflector and the embedded gains are mainly confined within a half space. In this case interesting results can be achieved by turning on that pair of ports having high gain in the required angular sector.

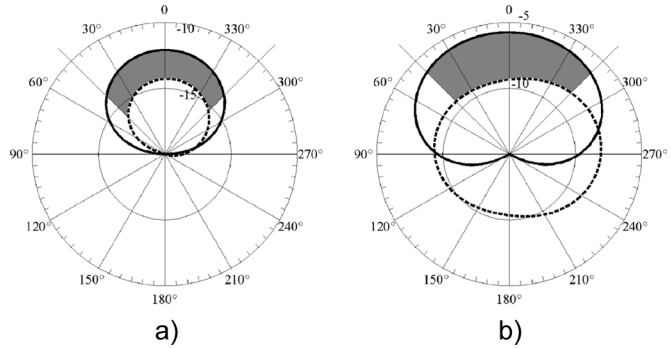

Fig. 11. Phased NSA_4 (continuous lines) for NVIS links around $\phi_0 = 0°$ at $\theta_0 = 10°$ compared with the embedded pattern having the highest gain at such a direction (dashed lines). (a) $f = 4$ MHz, two ports used, $\alpha_3 = \alpha_2$, $VSWR = 2.6$, $I = 63\%$. (b) $f = 6$ MHz, four ports used, $\alpha_1 = 0$, $\alpha_2 = 59°$, $\alpha_3 = 70°$, $\alpha_4 = 344°$, $1.9 < VSWR < 3$, $I = 108\%$.

C. Enhancement of NVIS Radiation

The multiobjective optimization of the NSA_N excitation is finally applied to the enhancement of the NVIS radiation which can be obtained within a given azimuthal direction by using a phased NSA_N. This feature can be useful when an obstacle, e.g., a mountain, prevents the sea-wave propagation in a given direction. The penalty function in (2) is customized by setting $w_A = w_U = 0$. As in the previous paragraph, the optimized results for the NSA_4 on the frigate model are compared with the embedded gain pattern having the best radiation in $|\phi - \phi_0| \leq 45°$ at $\theta_0 = 10°$ (Fig. 11). An average 3 dB improvement in the peak gain can be appreciated at the considered frequencies, while the radiated power has been nearly doubled.

VI. Conclusion

This work has demonstrated that, by using a proper design strategy, the multiport Naval Structural Antenna concept is still feasible in realistic naval environments. The shape of the wires feeding the naval superstructure may retain the same form than that found for the canonical geometry on a perfect ground. The impedance loading dislocation needs instead to be specifically designed for the particular installation typology and therefore an electromagnetic model of the whole ship is required.

Also the multichannel management is still possible with relevant improvement in the overall efficiency, but due to the embedded pattern nonuniformity, some care is required to allocate the channels to the best suited ports depending on the frequency and on the angular sector interested to the communication.

The proposed constrained pattern-shaping and port-matching design procedure permits different types of radiation patterns control with unconventional features in the case of both broadcast (uniform pattern) or sectorial coverage. In the last case, radiation power improvement from 50% up to 200% can be obtained in comparison with conventional single-port broadband antennas.

The resulting structure can be quite compact, about a 1 m larger than the mast base in the considered platform. The power supply and the transmitters can be therefore concentrated within a small space with a great simplification on the distribution and control networks. When equipped with the Software Defined Radio technology and the algorithms for antenna ports control,

the NSA_N framework seems therefore to promise most of the communication services demanded to the HF band with unparalleled flexibility and power saving.

Future work will consider the evaluation of manufactured scaled prototypes for some kinds of relevant ship superstructures.

APPENDIX

The detailed definitions of the penalty function components in (2) are here reported.

A. Matching Penalty F_S

$$F_S = \frac{1}{N_P}\sum_{i=1}^{N_P} p_S^{(i)} \tag{4}$$

$$p_S^{(i)} = \begin{cases} 0 & \text{if } VSWR^{(i)} < s_0 \\ \frac{VSWR^{(i)} - s_0}{VSWR^{(i)}} & \text{otherwise} \end{cases} \tag{5}$$

where N_P is the number of excited ports, $VSWR^{(i)}$ refers to the $i-th$ port and s_0 is a threshold value that has not to be exceeded (generally $s_0 = 3$ in the HF band).

B. Uniformity Penalty F_U

$$F_U = \begin{cases} 0, & \text{if } G_{EFF} > g_{TH} \\ \frac{g_{TH} - G_{EFF}}{g_{TH}}, & \text{otherwise} \end{cases} \tag{6}$$

$$G_{EFF} = G_{AV}U, \quad U = \frac{1}{N_\phi}\sum_{n=1}^{N_\phi} \delta_U(\phi_n) \tag{7}$$

$$\delta_U(\phi_n) = \begin{cases} 0, & \text{if } G_H(\phi_n) < \frac{G_{MAX}}{g_U} \\ 1, & \text{otherwise} \end{cases} \tag{8}$$

where $G_H(\phi_n)$ is the horizontal gain ($\theta = 90°$) along the ϕ_n direction, G_{MAX} is the maximum value of the G_H curve and g_U is a threshold value set on the basis of the uniformity requirement with respect to the maximum gain (a typical value is $g_U = 0.1$). N_ϕ is the number of points where the azimuthal gain is evaluated, U is the pattern uniformity, e.g., the percentage of the whole azimuthal angle where G_H meets the uniformity requirement, G_{AV} is the ϕ-averaged value of G_H, and G_{EFF} is an effective average gain which correctly penalizes those patterns that, although uniform in azimuth, exhibit a low average gain. Finally, $g_{TH} = u_{TH} \cdot g_{AV}$ is a threshold value for the effective gain G_{EFF}, where u_{TH} and g_{AV} are the desired values of the pattern uniformity function U and of the average gain G_{AV}, respectively.

C. Horizontal Gain Penalty F_A

$$F_A = \frac{1}{N_{\Delta\phi}}\sum_{n=1}^{N_{\Delta\phi}} p_A(\phi_n)$$

$$p_A(\phi_n) = \begin{cases} 0, & \text{if } G_H(\phi_n) > g_A \\ \frac{g_A - G_H(\phi_n)}{g_A}, & \text{otherwise.} \end{cases} \tag{9}$$

$N_{\Delta\phi}$ is the number of ϕ_n points in the angular sector $\Delta\phi$, centered at the ϕ_0 direction, where the horizontal gain G_H ($\theta = 90°$) has to be maximized. g_A is a threshold value establishing the desired gain level in such a angular sector.

D. NVIS Penalty F_V

The definition of F_V is the same as F_A with the NVIS gain $G_V(\phi_n)$ at $\theta = 10°$ instead of $G_H(\phi_n)$.

E. Excited Ports Penalty F_N

$$F_N = \frac{N_p - 1}{N - 1}. \tag{10}$$

N_p is the number of simultaneously excited ports of the NSA_N.

ACKNOWLEDGMENT

The authors wish to thank the Software Radio Team of Mr. G. Falcione for inspirations, and Prof. F. Bardati and Prof. P. Tognolatti for suggestions and valuable discussions.

REFERENCES

[1] J. Mitola, "The software radio architecture," *IEEE Commun. Mag.*, vol. 33, no. 5, pp. 26–38, May 1995.
[2] J. Mitola, III and Z. Zvonar, Eds., *Software Radio Technologies: Selected Readings*. New York: Wiley–IEEE Press, 2001.
[3] W. H. W. Tuttlebee, "Software-defined radio: facets of a developing technology," *IEEE Personal Commun. (see also IEEE Wireless Commun.)*, vol. 6, no. 2, pp. 38–44, Apr. 1999.
[4] J. V. N. Granger, "Shunt excited flat plate antennas with applications to aircraft structures," in *Proc. IRE*, Mar. 1950, vol. 38, no. 3, pp. 280–287.
[5] C. E. Baum, "Airframes as Antennas," in *Sensor and Simulation Notes*. Albuquerque, NM: Air Force Research Lab, May 1995, Note 381.
[6] G. Marrocco and P. Tognolatti, "New method for modelling and design of multiconductor airborne antennas," *Proc. Inst. Elect. Eng. Microw. Antennas Propag.*, vol. 151, no. 3, pp. 181–186, Jun. 2004.
[7] M. Anstey and S. A. Saoudy, "Radiation charactersitics of a ship-mounted high frequency ground wave radar antenna," in *Antennas Propag. Soc. Int. Symp.*, Jul. 1996, vol. 3, pp. 1852–1855.
[8] S. R. Best, "On the use of scale brass models in HF shipboard communication antenna design," *IEEE Antennas Propag. Mag.*, vol. 44, pp. 12–22, Apr. 2002.
[9] G. Marrocco and L. Mattioni, "Naval structural antenna system for broadband HF communications," *IEEE Trans. Antennas Propag.*, vol. 54, no. 6, pp. 1065–1073, Apr. 2006.
[10] G. Marrocco, L. Mattioni, F. Bardati, M. Proia, P. Tognolatti, R. Perelli, G. Colasanti, and G. Falcione, "Structural Broadband HF Antenna for Naval Installation," TO2005A000417, Italian patent pending.
[11] L. Mattioni and G. Marrocco, "BLADE: a broadband loaded antennas designer," *IEEE Antennas Propag. Mag.*, Oct. 2006.
[12] Z. Altman, R. Mittra, and A. Boag, "New designs of ultra wide band communication antennas using a genetic algorithm," *IEEE Trans. Antennas Propag.*, vol. 45, pp. 1494–1501, Oct. 1997.
[13] L. Mattioni and G. Marrocco, "Design of a broad-band HF antenna for multi-mode naval communications," *IEEE Antennas Wireless Propag. Lett.*, vol. 4, pp. 179–182, 2005.
[14] FEKO User's Manual, Suite 5.1 EM Software & Systems-S.A. (Pty) Ltd., Dec. 2005. Stellenbosch, South Africa [Online]. Available: http://www.feko.info
[15] C. C. Lu and W. C. Chew, "A multilevel algorithm for solving boundary-value scattering," *Micro. Opt. Tech. Lett.*, vol. 7, no. 10, pp. 466–470, Jul. 1994.
[16] J. Dresel, A. R. Clark, and A. P. C. Fourie, "Applying soft magnetic materials to conductive surfaces to realize a novel conformal HF antenna concept," in *IEEE AFRICON*, 1999, vol. 2, pp. 1069–1074.
[17] C. E. Baum, "Ship Platform for HF/VHF Arrays," in *Sensor and Simulation Notes*. Albuquerque, NM: Air Force Research Lab, Aug. 1995, Note 383.
[18] P. Hannan, D. Lerner, and G. Knittel, "Impedance matching a phased-array antenna over wide scan angles by connecting circuits," *IEEE Trans. Antennas Propag.*, vol. 13, no. 1, pp. 28–34, Jan. 1965.
[19] M. G. Bray, D. H. Werner, D. W. Boeringer, and D. W. Machuga, "Matching network design using genetic algorithms for impedance constrained thinned arrays," in *IEEE Antennas and Propagation Society Int. Symp.*, Jun. 2002, vol. 1, pp. 528–531.

[20] W. Kahn, "Impedance-match and element-pattern constraints for finite arrays," *IEEE Trans. Antennas Propag.*, vol. 25, no. 6, pp. 747–755, Nov. 1977.
[21] M. Shimizu, "Determining the excitation coefficients of an array using genetic algorithms," *IEEE Antennas Propagation Society Int. Symp.*, vol. 1, pp. 530–533, Jun. 1994.

Gaetano Marrocco (M'98) received the Laurea degree in electronic engineering and the Ph.D. degree in applied electromagnetics from the University of L'Aquila, Italy, in 1994 and 1998, respectively.

Since 1997, he has been a Researcher at the University of Rome "Tor Vergata," Rome, Italy, where he currently teaches antenna design and bioelectromagnetics. In summer 1994, he was at the University of Illinois at Urbana-Champain as a Postgraduate Student. In autumn 1999, he was a Visiting Researcher at the Imperial College in London, London, U.K. He has been involved in several space, avionic and naval programs of the European Space Agency, NATO, Italian Space Agency, and the Italian Navy. His research is mainly directed to the development of numerical methods and signal processing techniques for the time domain modeling and design of complex electromagnetic structures in the context of biological and aerospace applications.

Lorenzo Mattioni received the Laurea degree in telecommunications engineering from the University of Rome Tor Vergata, Italy, in 2004, where he is currently working toward the Ph.D. degree in electromagnetics.

In 2004, he was a Grant Researcher at the University of Rome Tor Vergata, working on broadband antennas for HF naval communications. His scientific interests are the modeling and design of innovative broadband antenna systems for mobile platforms and for the Software Defined Radio technology.

Valerio Martorelli received the Laurea degree in telecommunications engineering from the University of Rome Tor Vergata, Italy, with the thesis "Models of HF Antennas on Naval Plant."

From December 2005 to February 2006, he was with Electromagnetics Group at same university working on broadband naval antennas for HF applications. Since May 2006, he has been a Grant Researcher at the National Institute of Astrophysics of Bologna, Italy, where he focuses on the design of antennas and electromagnetic devices for UHF, X, and Ku applications.